AIAA 2001-0377
On the Role of Nonlinearity in Mach Wave Radiation in a Mach=1.92 Jet

K. Mohseni and T. Colonius
Division of Engineering and Applied Science
California Institute of Technology
Pasadena, CA 91125

J.B. Freund
Department of Mechanical and
Aerospace Engineering
University of California
Los Angeles, CA 90095

AIAA 2001-0377

ON THE ROLE OF NONLINEARITY IN MACH WAVE RADIATION IN A MACH = 1.92 JET

Kamran Mohseni Tim Colonius
Division of Engineering and Applied Science
California Institute of Technology
Pasadena, CA 91125

Jonathan B. Freund
Department of Mechanical and
Aerospace Engineering
University of California, Los Angeles, CA 90095

Abstract

Mach wave radiation in a turbulent fully expanded supersonic jet is revisited. Our goal is to determine the extent to which predictions for the radiated sound that are based on linearized analysis agree with solution of the full nonlinear equations. To this end, we solve the linearized Navier-Stokes equations (LNS) with precisely the same mean flow and inflow disturbances as a previous direct numerical simulation (DNS) of a turbulent $M = 1.92$ jet.[1] We restrict our attention to the first two azimuthal modes, $n = 0$ and $n = 1$, which constitute most of the acoustic field. The direction of peak radiation and the peak Strouhal number matches the DNS reasonably well, which is in accord with previous experimental justification of the linear theory. However, it is found that the sound pressure level predicted by LNS is significantly lower than that from DNS. Thus, linear theory misses a substantial component of the noise. In order to investigate the discrepancy, the behavior of individual frequency components of the solution are examined. Near the peak Strouhal number, particularly for the azimuthal mode $n = 1$, the amplification of disturbances in the LNS closely matches those from the DNS data. However, away from the peak frequency (and generally for the azimuthal mode $n = 0$), the DNS data shows amplification rates roughly comparable to those at the peak Strouhal number, while those from the linear computations are damped.

1 Introduction

In the last three decades one of the important developments in turbulent research was the recognition of large scale turbulent structures in free shear flows (see Brown and Roshko[2]). There is now a large body of evidence that connects the evolution of linear instability waves and large scale structure.[3-5] Furthermore, theoretical[6] and experimental[7] evidence suggests that the noise generated by large coherent structures constitutes the principal part of the supersonic turbulent mixing noise, which is thought to be Mach wave radiation that occurs when large structures convect at supersonic speed relative to the ambient.

Prediction of supersonic mixing noise has followed these ideas closely since the development of a linear stability noise models for mixing layers[8] and jets.[6] These theories use matched asymptotic expansions (MAE), to expanded the near-field solution of the linearized flow equations with the spreading rate as a small parameter and match this expansion to a global solution to the wave equation in the far field. Tam and Burton[6] show that the peak Strouhal number of the radiated sound and the directivity pattern of the most amplified linear mode match the jet noise measurements of Troutt and McLaughlin.[7]

Unfortunately, the noise amplitude predicted by a linear theory is directly proportional to the amplitude of the fluctuations at the nozzle lip which are typically unknown. A rigorous prediction of the noise amplitude based on actual nozzle disturbances has never been performed. So to predict noise, additional assumptions about the excitation of linear modes are required. For example, the stochastic wave model developed by Tam and Chen[9] considers a single instability wave at any given frequency as representative of the energy carrying wave component (that is, it neglects the continuous spectrum of convected disturbances). They argue that the instability wave spectrum of the jet may be regarded as being generated by the stochastic white noise excitation at the nozzle lip region. Thus the amplitude of instability waves are set by matching the turbulent kinetic energy of the flow at the nozzle lip.

Several important questions regarding the stochastic wave model have yet to be addressed are: (1) how important is the continuous spectrum of disturbances, either by itself or in combination with the instability modes; (2) to what extent

do nonlinear interactions regulate the growth and decay of the instability waves; and (3) is the linear mechanism of Mach wave generation the dominant sound source, or is sound generated by interactions of waves significant?

Recently, a turbulent unheated jet at a Mach number of 1.92 was computed using Direct Numerical Simulation (DNS) by Freund, Lele & Moin.[1] Though the Reynolds number was low ($Re = 2000$), it was shown that the directivity and SPL were similar to higher Reynolds number jets with similar convective Mach numbers. This DNS provides a detailed database that can be used to address the above questions. In a related paper, Colonius and Freund[10] used the database to show that there was quantitative agreement between the acoustic field directly computed in the DNS and that found by solving the wave equation with a Lighthill source term that was computed from the DNS data.

In the present paper, we compare these DNS results with numerical solutions of the Linearized Navier-Stokes (LNS) equations, with the mean flow taken directly from the DNS and with precisely the same inflow disturbances. This provides, then, the first direct assessment of nonlinearity in determining the amplitude of the radiation. The paper is organized as follows. In the next section, the computational technique and issues relating to signal analysis of the data are briefly described. A more detailed account of these issues is available elsewhere.[11] Results are presented and discussed in section 3, and a summary of our conclusions is given in section 4.

2 Computational Technique

A linearized Navier-Stokes solver was developed that uses the mean flow quantities, grid distribution and inflow boundary conditions, including an identical specification of incoming turbulent disturbances, from the Freund *et al.*[1] simulation. It uses a sixth-order compact Padé scheme in axial and radial direction and a Fourier spectral method in the azimuthal direction, and a fourth-order Runge-Kutta algorithm to advance the solution in time.

It is currently not computationally feasible to simultaneously simulate the nozzle flow as well as the small-scale turbulence and the far-field acoustic waves by DNS. Therefore, inflow conditions were used to mimic the behavior of the shear layer a short distance downstream of the nozzle, and we use the identical specification as input to the LNS computations. The inflow condition developed by Freund[12] is based on an auxiliary DNS computation of a periodic (temporally evolving) jet.[13,14] This simulation had a streamwise period of $21R$, where R is the jet radius at the inlet. In order to decorrelate the turbulence of the incoming flow, the amplitude of the two-dimensional spectral components of the incoming disturbances were randomly jittered by an amount of 5% of their amplitude. The decorrelation of the small scale (high frequency) turbulence statistics within the computational domain was verified *a posteriori*. For some of the low frequency results presented in this paper, remnants of the $21R$ periodicity remain in the DNS data. This is expected in free shear layers that are known to be sensitive to initial conditions, and will take them a long distance for large scales to decorrelates in flow direction. In the LNS calculations, such correlation persists indefinitely since there is no exchange of energy with smaller scales. We note that while the details of the results here are affected by this correlation, the conclusions remain valid since we are comparing the relative evolution of two flows with identical inflow disturbances.

The flow parameters in the LNS calculations are set to their corresponding values in the DNS calculation. These are:

$$Pr = 0.7, \qquad \frac{T_\infty}{T_j} = 0.89,$$

$$Re_j = \frac{\rho_j U_j D_j}{\mu_j} = 2000, \qquad M = \frac{U_j}{a_j} = 1.92.$$

The isentropic convective Mach number[15] for these conditions is $M_c = 0.99$, the momentum thickness of the incoming shear layer is $0.1R$, and the computational domain extends $13.3R$ in the radial direction and $36R$ in the axial direction, see figure 1. The computational mesh for the DNS calculation had $640 \times 270 \times 128$ points in the axial, radial, and azimuthal directions, respectively. We found that in LNS calculations full resolution in the axial direction and half resolution in the radial direction provided results that were essentially identical to those computed with the DNS resolution. Since the acoustic field from DNS was dominated by the first two azimuthal modes (see below) we use only 4 points in the azimuthal direction, noting that higher azimuthal modes are completely decoupled in linear computations.

To avoid problems with the polar coordinate singularity, the centerline treatment proposed by Mohseni and Colonius[16] is used, where singular coordinates are redefined so that data is differentiated smoothly through the pole, and we avoid placing a

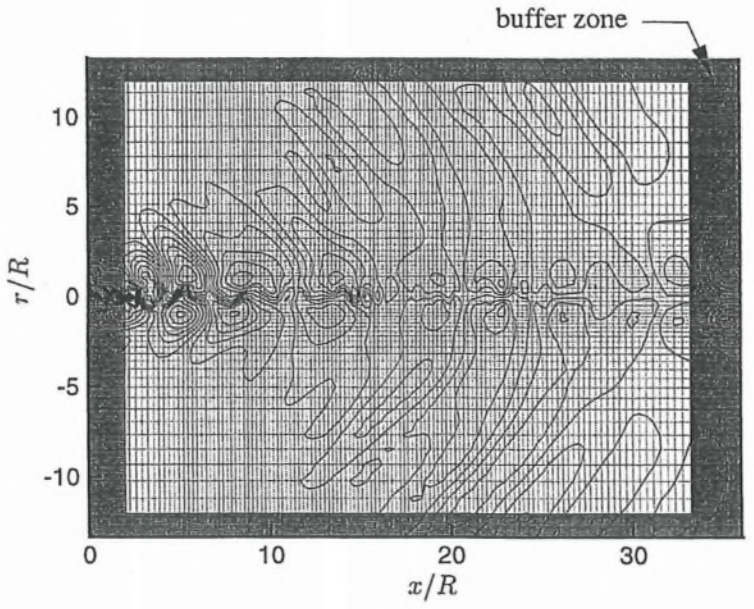

Figure 1: Computational domain and buffer zones.

grid point directly at the pole. This eliminates the need for any pole equation. In this technique the locations of radial grids in the LNS computational domain are placed half way between the grid points of the DNS calculations. For this reason, a fourth-order compact Padé mid-point interpolation formula was used to transform all the flow data, inflow boundary conditions and mean flow distributions in the DNS calculations to the radial grids of the LNS calculations.

2.1 Signal Processing Techniques

In this section methods for extracting frequency spectra from the LNS and DNS data are considered. Due to the different nature of data in each case, different methods are used:

Discrete Fourier Transform: Since the quasi-periodicity is quite evident in the LNS calculations the Fourier spectra were calculated using standard discrete Fourier methods. Apart from the aperiodicity imposed on the inflow boundary condition, aperiodic behavior of the data can be caused by many other factors, including existence of signals with frequencies too low to be represented over a specific duration of signal and also signals with frequencies higher than the Nyquist frequency of the sampled data. The approximate spatial periodicity of the inflow data can be translated into temporal periodicity with a period $Ta_\infty/R = 21$ (assuming a convection speed of unity, which is appropriate at these flow conditions). The total duration of the LNS data was to $3Ta_\infty/R$. The LNS calculations are at an almost periodic state after the first flow through the entire computational domain. Our numerical experiments show that even one period of the LNS data is enough to accurately calculate the spectra at the smallest frequency, $fR/a_\infty = 1/21$, and increasing the period Ta_∞/R did not change the results.

The LNS data is sampled every time step to avoid aliasing. The resulting sampling rate was $fR/a_\infty = 100$, which is well above the maximum frequency considered in this study.

Lomb-Scargle Periodogram: While the direct Fourier transform was quite accurate for calculating the frequency spectra of the evenly sampled data from the LNS computations, it would not be reliable in the case of DNS data because of several computational issues. Though the DNS data is quasi-periodic near the inflow, it is fully aperiodic further downstream. Thus, imposing a periodicity here would contaminate the high frequencies. In addition, the DNS data were computed with a variable time step, and there were a few short-duration patches of missing DNS data. There are 2496 samples between computational times $156R/a_\infty$ and $352R/a_\infty$, constituting more than 9 periods of the inflow forcing. This

is sufficient to show that the data is more than sufficient for the frequencies of interest.

An efficient technique that can be applied to unequally sampled data, which also includes regular time-series with missing values is the Lomb-Scargle periodogram.[17,18] While a Fourier transform decomposes the time-series into a fundamental periodicity and a number of harmonics, a periodogram shows the power of each of these periodicities and was developed to detect weak periodic signals in noisy data. The fast algorithm for computing the the Lomb-Scargle spectrum of Press *et al.*[19] was used.

Since the sampling theorem applies only to evenly sampled data, the Nyquist frequency is not defined for the unevenly sampled DNS data. Nevertheless, an average Nyquist frequency can be defined as

$$\bar{f}_N = \frac{1}{2\overline{\Delta t}}, \tag{1}$$

where $\overline{\Delta t}$ is the average sampling interval. Usually choosing the maximum frequency of interest to be this average Nyquist frequency results in a conservative choice of frequency range. The average Nyquist frequency for the available DNS data is almost $13a_\infty/R$, and is well above the highest frequencies considered in this study.

3 Results

3.1 Sound Pressure Level

We begin by computing the sound pressure level (SPL) of the DNS and LNS data at $r = 12R$, which is the maximum extent of the DNS. The results of this computations are presented in figures 2 and 3 for both DNS and LNS.

There are several features to note in these figures. First, the acoustic field of the DNS data is dominated by modes zero and one. When all other modes are excluded, the total SPL is reduced by only 1.5 dB. This confirms the predictions from linear stability theory (LST) that the acoustic field of a cold jet (and relatively cold jets) is dominated by the first two modes.[20] Because of this, we limit our attention in what follows to only the first two modes. Second, in agreement with predictions from LST,[20] the azimuthal mode $n = 1$ in the LNS calculation contributes the most to the total SPL and is clearly the dominant part of the generated noise. However, the same trend is not observed in the DNS data. The maximum SPL of the DNS data for $n = 0$ alone is actually higher than that of mode $n = 1$ and cannot

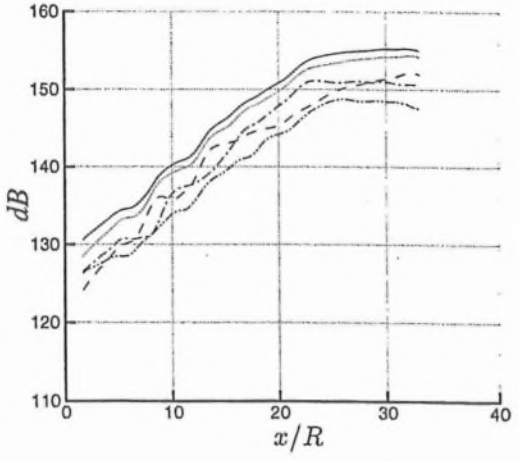

Figure 2: SPL of DNS at $r = 12$. (———) total; (- - - -) $n = 0$ mode zero; (— · —) $n = 1$ mode; (·····) both $n = 0$ and 1 modes; (— ·· —) all other modes.

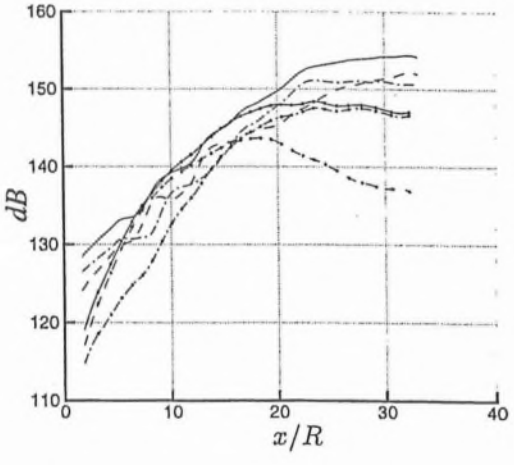

Figure 3: SPL at $r = 12$. For DNS: (———) sum of modes $n = 0$ and 1; (- - - -) $n = 0$; (— · —) $n = 1$, and for LNS: (—•—) sum of modes $n = 0$ and 1; (- - •-) $n = 0$; (—•—) $n = 1$.

be ignored, while in the LNS calculations considering only $n = 1$ provides a reasonable estimate for the total SPL. Contrary to LNS and LST calculations, the radiation from mode $n = 0$ in the DNS peaks further downstream than it does for mode $n = 1$. This can be interpreted to mean that the apparent location of the sound sources of mode $n = 0$ of the DNS calculation is concentrated further away from the nozzle. Since the inflow data for both LNS and DNS are exactly the same, this effect cannot be attributed to any artificiality of the inflow forcing.

In both LNS and DNS, the acoustic field is highly directional. For $n = 1$ the general directivity profile is well captured, while its amplitude is underestimated by as much as 4dB at $r = 12$. The agreement is poorer for $n = 0$, where LNS data is less intense by as much as about 15 dB. Because azimuthal mode $n = 1$ contributes the most to the total SPL of the LNS calculations, the total directivity of the LNS data does follow the directivity of the total SPL from the DNS calculation closely. However, the maximum SPL of the sum of modes $n = 0$ and $n = 1$ is underestimated by as much as 8 dB in the LNS calculation. It is clear that some noise mechanism is not represented by the linear equations.

Note that these amplitude comparisons are performed outside the jet, but only at $r = 12R$. Shocks in the sound field[1] will increase dissipation of the noise so one might expect a somewhat better agreement at a larger distance from the jet, but this can not explain the 8 dB difference at $r = 12$.

3.2 Instantaneous Fields

Instantaneous pressure fields of the DNS and LNS data for $n = 0$ and 1 are shown in figure 4. There is a region of agreement between DNS and LNS for both $n = 0$ and $n = 1$ in a region close to the inflow boundary. This region of extends further downstream for $n = 1$ than it does for $n = 0$, which is consistent with the better match in amplitude discussed in the previous section, but gradually deteriorates further downstream. Disagreement is expected, especially in the near field, since these instantaneous observations contain all frequencies, and the DNS data has a broader spectrum. This is evident in the DNS data of figures 4(a,c,e) where smaller scales are observed that are absent in the LNS calculations of figure 4(b,d,f). Consequently, around the end of the potential core the LNS calculation is not a good representative of the fluctuations in the DNS data. However, it appears that on an instantaneous basis, the LNS qualitatively captures that sound radiation that mainly originates from near the nozzle.

It seems that the highest amplitude Mach wave radiation for $n = 0$ of the LNS data originates from an area close to the inflow boundary (close to the nozzle exit) while for $n = 1$ it radiates from a region around $x \approx 7R$ and extends beyond the end of the potential core. This clearly affects the directivity of the near acoustic field for $n = 0$ and 1. While a distant far-field observer will not distinguish this shift in the location of the apparent source, it is clear at $r = 12R$, as seen in figure 3, where the SPL of the zero azimuthal mode of the LNS data at $r = 12R$ peaks earlier that that of mode one. Thus LNS computations provide a picture consistent with linear stability theory. On the other hand, the DNS appears to have contributions from both the shear layer region, and from a region near the end of the potential core.

3.3 Amplification of individual frequency components

The comparison of the sound pressure levels and instantaneous pressure levels in the last two sections showed that the linearized computations radiate less, especially from the axisymmetric mode, $n = 0$. Instantaneous pressure contours showed that the intense Mach wave radiation from a region near the end of the potential core in the DNS was not captured by the LNS. However, linear instability modes are only expected to model the largest scales. Because the DNS jet is at a low Reynolds number, too low to have an appreciable inertial range in the turbulence cascade, we do not expect significant contribution to the noise from other than the largest scales. Nevertheless, it remains unclear whether the discrepancies noted in the previous sections are due to the generation of higher frequencies in the DNS, which despite its low Reynolds number does have broad-banded turbulence spectra, or whether there is error even at low frequencies. For this reason the DNS and LNS data were time transformed as discussed in section 2. The spatial development of the pressure disturbances at various Strouhal numbers (fD/U_j) in the DNS calculation is compared with the LNS calculation in figures 5 and 6* for $r = 1R$ and $r = 4R$. We see that at all frequencies the amplitudes agree at the inflow boundary, as expected since identical inflow forcing was used for both cases. Excellent prediction of the growth is ob-

*$\tilde{p} = (\tilde{p}_r^2 + \tilde{p}_i^2)^{1/2}$, where $\tilde{p}_r$ and $\tilde{p}_i$ are the amplitudes of the Fourier coefficients of the real and imaginary parts of the first azimuthal mode, respectively.

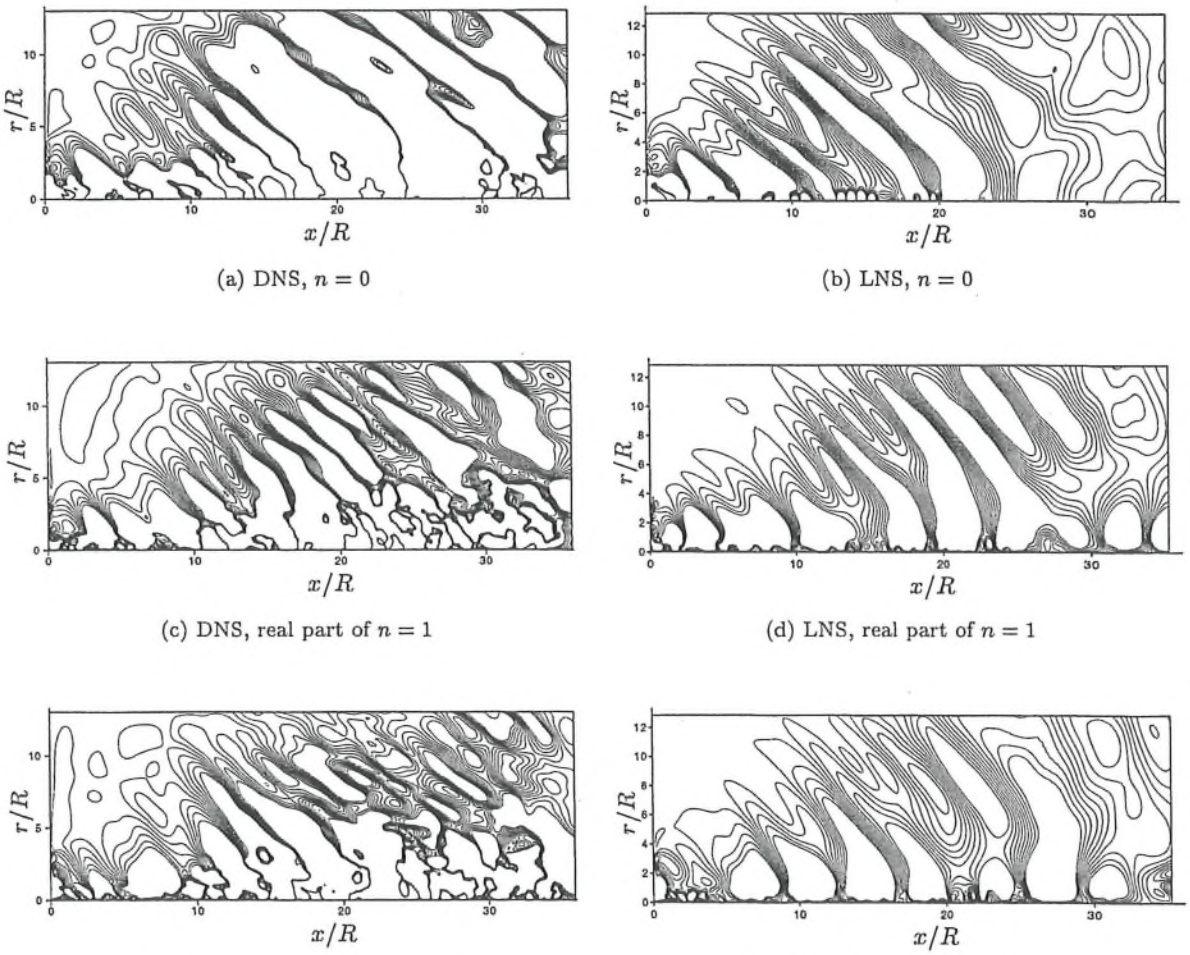

(a) DNS, $n = 0$

(b) LNS, $n = 0$

(c) DNS, real part of $n = 1$

(d) LNS, real part of $n = 1$

(e) DNS, imaginary part of $n = 1$

(f) LNS, imaginary part of $n = 1$

Figure 4: Instantaneous perturbation pressure field from DNS and LNS at time 222, normalized with $\rho_\infty a_\infty^2$. 10 contour levels between -0.00225 and 0.00225.

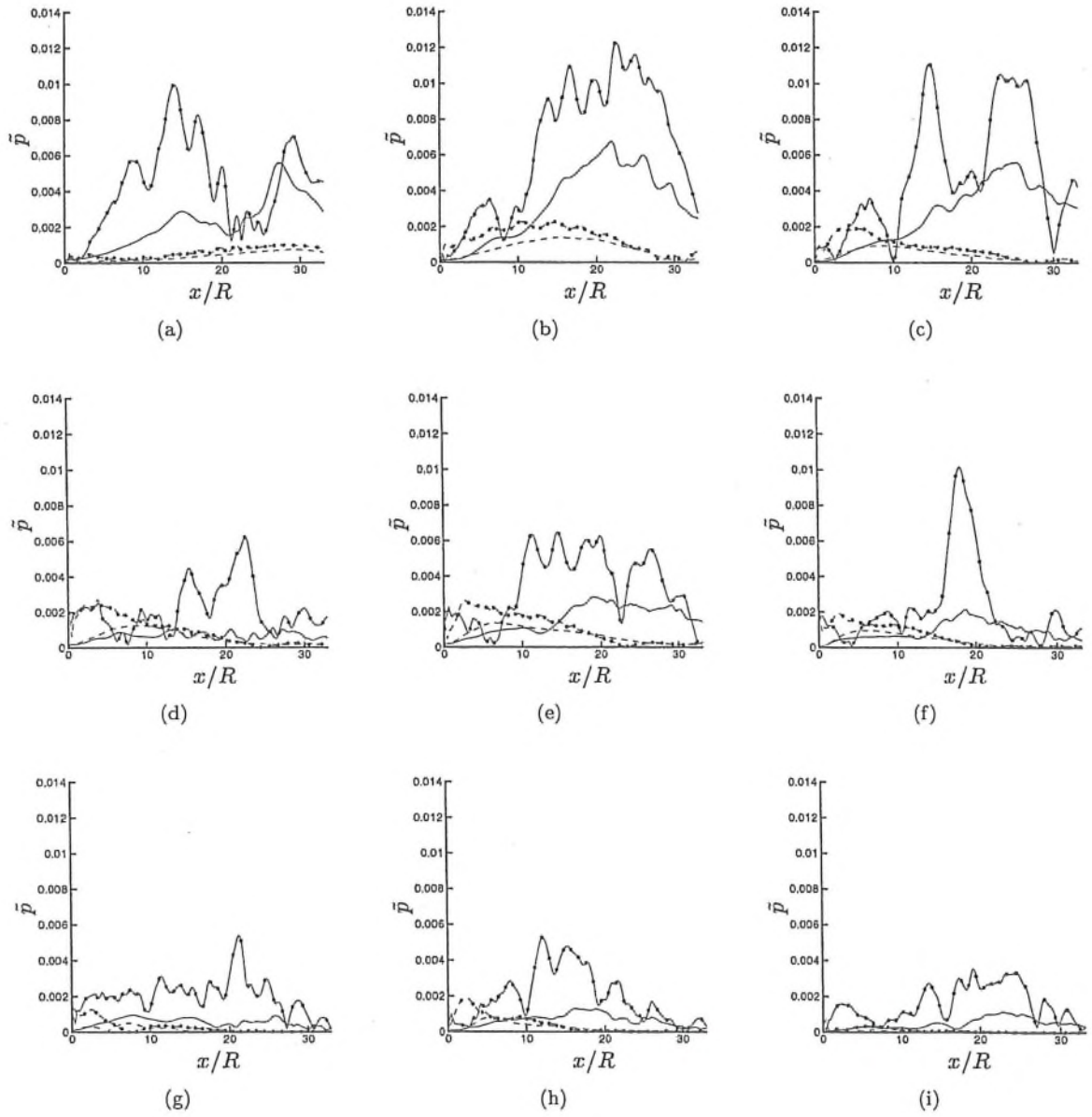

Figure 5: Amplitude of the Fourier coefficient for perturbation pressure field for $n = 0$, normalized with $\rho_\infty a_\infty^2$, for (a) $St = 0.048$ (b) $St = 0.095$ (c) $St = 0.143$ (d) $St = 0.191$ (e) $St = 0.238$ (f) $St = 0.286$ (g) $St = 0.333$ (h) $St = 0.381$ (i) $St = 0.429$. (—•—), DNS at $r = 1$; (--•-), LNS at $r = 1$; (——), DNS at $r = 4$; (----), LNS at $r = 4$.

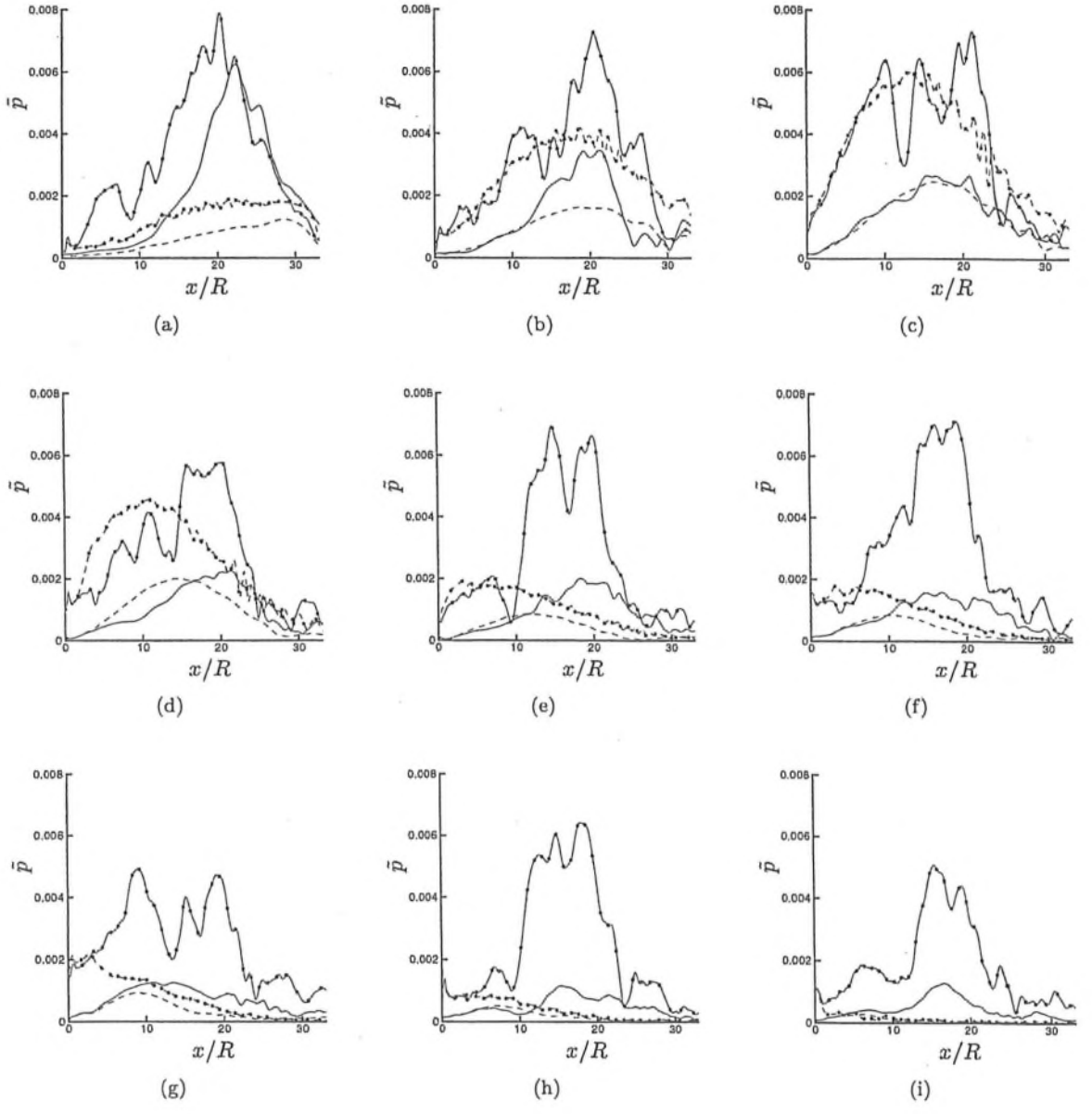

Figure 6: Amplitude of the Fourier coefficient for perturbation pressure field for $n = 1$, normalized with $\rho_\infty a_\infty^2$, for (a) $St = 0.048$ (b) $St = 0.095$ (c) $St = 0.143$ (d) $St = 0.191$ (e) $St = 0.238$ (f) $St = 0.286$ (g) $St = 0.333$ (h) $St = 0.381$ (i) $St = 0.429$. (—•—), DNS at $r = 1$; (--•-), LNS at $r = 1$; (———), DNS at $r = 4$; (----), LNS at $r = 4$.

served for mode $n = 1$ at $St = 0.143$ (figure 6 c), which is near the peak, and reasonable agreement is seen at similar Strouhal numbers in the range $0.0952 \lesssim St \lesssim 0.1905$. But in most cases, the fluctuations from LNS start to decay closer to the inflow, and with significantly lower amplitude than the corresponding fluctuations from DNS. In all cases, the agreement between DNS and LNS is better for $n = 1$ than it is for $n = 0$, which is consistent with the instantaneous and root-mean-square results presented above.

Another general trend in figure 6 is that the higher frequencies of the LNS calculation saturate earlier than the lower frequencies, an effect which is consistent with linear stability theory, but not evident in the DNS.

The observation that turbulence near the end of the potential core is responsible for a portion of the Mach wave radiation is not new. It was observed experimentally by Troutt and McLaughlin,[7] where the near acoustic field suggested that there were two distinct sources at a given frequency, one originating from the shear layer region, the other further downstream. In the present low Reynolds number simulation, the shear layers are initially thick enough frequencies above $St = 0.4$ are damped immediately, which we believe obscures this two-source effect. The noise from the shear layers and from further downstream cannot be clearly distinguished.

4 Discussion and Summary

In this study we have critically evaluated the linear theory of Mach wave radiation in a perfectly expanded supersonic jet. The relative directivity of the noise radiation predicted by linear computation was very similar to that obtained using DNS, but the noise radiated by the first two modes in the linearized computation was substantially weaker. For example, in the near acoustic field at a distance of 6 jet diameters from the jet centerline, the sound pressure level in the linearized computation was as much as 8 dB smaller in the linear solution. The first azimuthal mode, which is dominant in the linear theory, agreed better with the DNS than the axisymmetric mode which was substantially under predicted. In order to assess the origin of the discrepancy, frequency spectra were computed from both the DNS and LNS data. At the peak Strouhal frequency, particularly for $n = 1$, the amplification of disturbances in the LNS matched that of the DNS data. However, for other frequencies the DNS data showed amplification rates comparable to those of the peak Strouhal number, whereas in the LNS data the disturbances away from the peak Strouhal number were damped. Except near the peak frequency, the peak perturbations at a particular frequency in the DNS data occurred further downstream than for the LNS data, corresponding to a region around and beyond the end of the potential core.

Until present, evidence supporting the linear theory of Mach wave radiation was indirect: the general agreement of the directivity of the Mach wave radiation and its peak Strouhal number. In addition, the study of Troutt and McLaughlin[7] showed that the initial growth rates of the jet instabilities and the wavelengths of the coherent disturbances are in good agreement with linear stability theory predictions. While strikingly successful in predicting these important qualitative aspects of the noise, the present comparison shows that the noise process in not well modeled quantitatively by linear theory even if no further approximations, such as a slowly spreading mean flow, are made. Nonlinear effects are not only present, but they dominate the acoustic field for the axisymmetric mode $n = 0$, and contribute significantly to the $n = 1$ mode at frequencies different from that of the peak radiation. While the present analysis is restricted to low Reynolds number, there is no reason to expect that nonlinear effects and the discrepancy between the far-field sound pressure level and linear stability predictions, would be less important at high Reynolds number. Further, the missing noise in the linear theory must be attributed to nonlinearity, since inflow disturbances and the mean flow were exactly the same in both our linear and nonlinear calculations. However, we are not able to ascertain, based on the present results, whether it is due to a failure of linear theory to correctly predict the amplification of disturbances in the near field, or whether it is nonlinear mechanisms for sound radiation (or both).

It is not surprising that the directivity of the acoustic field near the peak Strouhal number is insensitive to the details of the source process. Indeed, the growth and decay of any constant frequency convecting disturbance will produce such radiation, albeit at an amplitude which depends critically on the growth and decay rates of the disturbance with streamwise distance. The present results show that except for the most amplified linear modes, the dominant sources arise further downstream and as the result of a nonlinear process, even though they produce similar overall directivity to the purely linear modes. This result suggests that linear theory for

Mach wave radiation should be used with caution. It may help explain why attempts to control the sound either by direct forcing of the flow, geometrical changes to the nozzle, or modification of any co-flow, may result in smaller reductions than would be predicted based on linear theory.

In order to complete the theory of Mach wave radiation from supersonic jets, and thereby produce a realistic model on which future noise control efforts could be based, future studies should concentrate on elucidating the mechanism by which nonlinear effects generate sound in the region near the end of the potential core.

References

[1] J.B. Freund, S.K. Lele, and P. Moin. Direct simulation of a Mach 1.92 jet and its sound field. to appear AIAA J., 2000.

[2] G. Brown and A. Roshko. On density effects and large structure in turbulent mixing layers. *J. Fluid Mech*, 64:775–816, 1974.

[3] D. G. Crighton and M. Gaster. Stability of slowly divergin jet flow. *J. Fluid Mech*, 88(2):397–413, 1976.

[4] M. Gaster, E. Kit, and I. Wygnanski. Large-scale structures in a forced turbulent mixing layer. *J. Fluid Mech*, 150:23–39, 1985.

[5] D. Oster and I. Wygnanski. The forced mixing layer between parallel streams. *J. Fluid Mech*, 123:91–130, 1982.

[6] C.K.W. Tam and D. Burton. Sound generation by instability waves of supersonic flows. Part 2. Axisymmetric jets. *J. Fluid Mech*, 138:273–295, 1984.

[7] T.R. Troutt and D.K. McLaughlin. Experiments on the flow and acoustic properties of a moderate-Reynolds-number supersonic jet. *J. Fluid Mech*, 116:123–156, 1982.

[8] C.K.W. Tam and P.J. Morris. The radiation of sound by the instability waves of a compressible plane turbulent shear layer. *J. Fluid Mech*, 98:349–381, 1980.

[9] C.K.W. Tam and P. Chen. Turbulent mixing noise from supersonic jets. *AIAA J.*, 32(9):1774–1780, 1994.

[10] T. Colonius and J.B. Freund. Application of Lighthill's equation to Mach 1.92 turbulent jet. *AIAA J.*, 38(2):368–370, 2000.

[11] K. Mohseni. *A: Universality in Vortex Formation B: Evaluation of Mach Wave Radiation in a Supersonic Jet.* PhD thesis, California Institute of Technology, April 2000.

[12] J. B. Freund. A proposed inflow/outflow boundary condition for direct computation of aerodynamic sound. *AIAA J.*, 35(4):740–742, 1997.

[13] J.B. Freund, P. Moin, and S.K. Lele. Compressibility effects in a turbulent annular mixing layer. Technical Report TF-72, Dept. Mech. Eng., Stanford University, Stanford, California, September 1997.

[14] J.B. Freund, S.K. Lele, and P. Moin. Compressibility effects in a turbulent annular mixing layer. Part 1. Turbulence and growth rate. *J. Fluid Mech.*, 421:229–267, 2000.

[15] D. Papamoschou and A. Roshko. The compressible turbulent shear layer: an experimental study. *J. Fluid Mech*, 197:453–477, 1988.

[16] K. Mohseni and T. Colonius. Numerical treatment of polar coordinate singularities. *J. Comp. Physics*, 157(2):787–795, 2000.

[17] N.R. Lomb. Least-squares frequency analysis of unequally spaced data. *Astrophysics Space Science*, 39:447–462, 1976.

[18] J.D. Scargle. Studies in astronomical time series analysis. II. Statistical aspects of spectral analysis of unevely spaced data. *Astrophys J.*, 302:757–763, 1982.

[19] W.H. Press, S.A. Teukolsky, W.T. Vetterling, and B.P. Flannery. *Numerical Recipes.* Cambridge Univ. Press, 2nd edition, 1992.

[20] C.K.W. Tam, P. Chen, and J.M. Seiner. Relationship between instability waves and noise of high-speed jets. *AIAA J.*, 30(7):1747–1752, 1992.